

Determination of the Stress and Resistivity of Stainless Steel Foams

Ahmed Telba *Member, IAENG, Member IEEE*, Mohamed Shehata Aly

Abstract— Over the past few years a number of low cost metallic foams have been produced and used as the core of sandwich panels and net shaped parts. The main aim is to develop lightweight structures which are stiff, strong, able to absorb large amount of energy and cheap for application in the transport and construction industries. For example, the firewall between the engine and passenger compartment of an automobile must have adequate mechanical strength, good energy and sound absorbing properties, and adequate fire retardance. Metal foams provide all of these features, and are under serious consideration for this applications by a number of automobile manufacturers (e.g., BMW and Audi). Additional specialized applications for foam-cored sandwich panels range from heat sinks for electronic devices to crash barriers for automobiles, from the construction panels in lifts on aircraft carriers to the luggage containers of aircraft, from sound proofing walls along railway tracks and highways to acoustic absorbers in lean premixed combustion chambers. But there is a problem. Before metallic foams can find a widespread application, their basic properties must be measured, and ideally modeled as a function of micro structural details, in order to be included in a design. This work aims at reviewing the recent progress and presenting some new results on fundamental research regarding the micromechanical origins of the mechanical, thermal, and acoustic properties of metallic foams in this paper after measuring all mechanical measurements we measure the electrical properties of the spasm material. In this paper adding new terms of measurements for electrical properties of the metal foams the main work adding the resistivity of the metal using four point probe the table of resistivity for attached.

Index Terms— metal foams, yielding, heat transfer, sound absorption, constitutive modeling, Electrical resistivity

I. INTRODUCTION

THIS paper includes two main parts first study the engineering materials the second part is the electrical property of the engineering materials. Recently, a new class of engineering materials, known as metal foams, has been developed. Metal foams show a wide range of features, for example high potential to absorb impact energy, high air and water permeability and good acoustic insulating properties. All these properties and more make them alternatives for applications in various significant fields like bioengineering, aerospace, automotive industries [1].

Manuscript received March 23, 2015; revised Manuscript received; revised April 7, 2015. Ahmed Telba is with King Saud university Electrical Engineering Department Saudi Arabia (corresponding author e-mail: atelba@ksu.edu.sa). Mohamed Shehata Aly is a researcher at Central Metallurgical Research & Development Institute, Helwan Cairo, Egypt.

Despite foams' increasingly importance, studies correlating their mechanical properties with the microstructure are still limited [2]. The compressive mechanical properties of metal foams were extensively investigated, as their applications concentrate mainly in construction and energy absorption. To spread their applicability, a deep understanding of the foams' properties under tension is needed. The present work aims at exploring the deformation behavior of open cell stainless steel foams under tension and studying comprehensively the effect of porosity, cell wall thickness on their mechanical properties. To do that, we carried out a series of tensile tests on open cell stainless steel foams with relative densities of 0.181, 0.050 and 0.037 and average pore sizes of 150, 300 and 600 μm , respectively. A measuring technique based on implementing a laser CCD camera was used to measure the tensile properties. The average fracture stress of the individual cells was statistically measured by using the Weibull distribution function.

Electrical resistance heating is a widely used technology to convert the electrical energy to thermal energy. The resistance to electrical current in a heating element generates heat. This heat is transferred to air flowing through the heating element. This study investigates the use of four point probe to calculate the electrical resistance of the element.

The resistance of a given sample will increase with the length, but decrease with greater cross-sectional area. Resistance is measured in ohms. Length over area has units of 1/distance. To end up with ohms, resistivity must be in the units of "ohms * distance" (SI ohm-meter, US ohm-inch). In a hydraulic analogy, increasing the cross-sectional area of a pipe reduces its resistance to flow, and increasing the length increases resistance to flow (and pressure drop for a given flow).

The electrical resistivity of each metal foam was determined using foam cut from the same sample as the corresponding heating element. Direct electric current was passed through a rectangular length of foam. The voltage and current were recorded, and the resistance calculated using Ohm's law. The physical dimensions of the test specimen, length, width, and thickness, were measured. From these parameters, the resistivity was determined

II. EXPERIMENTAL WORK

A. Materials & Equipment

In the present work, the tensile mechanical properties of three samples of open cell stainless steel foams with

different densities and average pore sizes, namely 150, 300 and 600µm respectively, were investigated. The foam samples were fabricated by a powder metallurgical method at Mitsubishi Materials Corporation in Japan. The procedure of the manufacturing process is explained in more detail in [3]. The samples hereafter will be noted as A, B and C. Table 1 shows the density, cell wall thickness and the porosity measurements of foam samples A, B and C, respectively. Fig. 1 shows a typical morphology of the open cell foam structure.

TABLE 1
 SHOWS THE DENSITY, CELL WALL THICKNESS AND THE POROSITY
 MEASUREMENTS OF FOAM SAMPLES A, B AND C

Specimen	Av. Thickness mm	Av. Cell Wall Thickness mm	Density g/cm ³	Porosity %
A	0.5	112.2	1.4	82
B	1	50.4	0.4	95
C	2	44.5	0.3	97

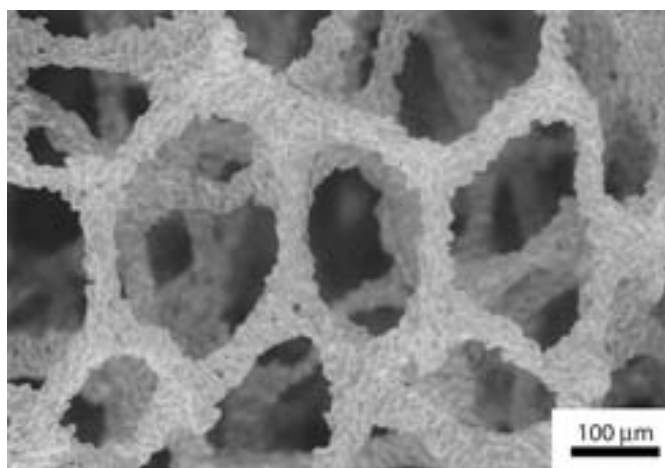


Fig. 1 Typical pore morphology of open cell foams.

Optical micrographs shown in Fig. 2 reveal the typical morphology of the open cell foams for samples A, B and C and their pore size distribution frequency. These micrographs were taken by a digital microscope KEYENCE VHX-500.

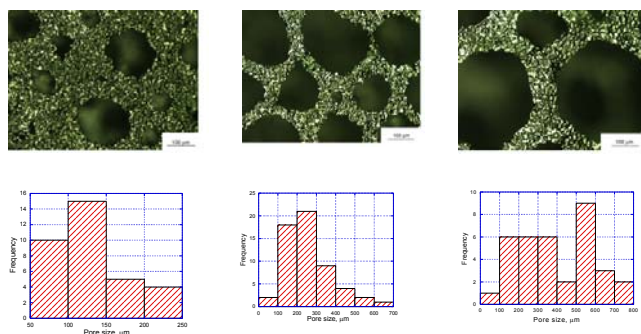


Fig. 2. Optical micrographs of pore structure and the pore size distribution frequency of foam samples A, B and C, respectively.

A universal testing machine Autograph AG-50 kNG, Shimadzu with a load cell of 200 N was used to perform the tensile tests. The tests were conducted at room temperature at a constant crosshead speed of 0.5 mm/min which matches a nominal strain rate of $1.7 \times 10^{-4} \text{ s}^{-1}$. Samples prepared for the tensile test have a rectangular shape with a cross-sectional area of 100 x 10 mm², and a gauge length of 50mm determined by black markers as shown in Fig. 3. The ends of the tensile samples are glued to aluminium tabs (with holes of 5mm in diameter), through which the load is transferred to the sample.

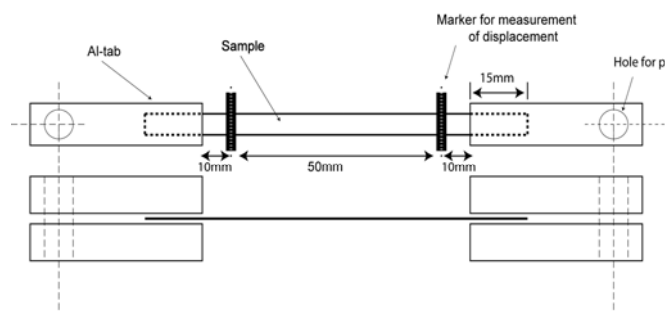


Fig. 3. A schematic sketch for the tensile test sample with aluminum tabs

Work function based on the usage of a laser CCD camera (DVW- 200 Shimadzu)

To avoid any deflection or deformation that can occur to the samples prior to testing, a non- contact laser extensometer was used to measure the resulting strain. The work function of this extensometer is based on the usage of a laser CCD camera (DVW- 200 Shimadzu).

Evaluating the test results is based on the average of 2 samples of each type. Fracture surfaces of foam samples were examined by a scanning electron microscope SEM (Jeol, JSM-5410LS) equipped with Electron Probe Micro-Analyzer (EPMA) (HITACHI, S3500).

B. RESULTS & DISCUSSION

Tensile Test

The outcome of the tensile test is represented by a typical stress-strain curve, as shown in Fig. 4. Three regions can be distinguished, linear elastic, strain hardening region as well as fracture region. The elastic region commences as the loading starts and continues with increasing the load until the yield point is reached. At the yield point, the sample begins to deform plastically. The stress- strain curve ends when the fracture occurs. The point at which the stress-strain curve stops is known as the fracture stress. At such stress the struts of the foam are no longer be able to bear more applied loads. The strain, at which fracture takes place, is known as the fracture strain. The fracture in all samples occurred successively following a zigzag line, as shown in Fig. 4. It can be noticed that samples (A) with the smallest pore sizes exhibited the largest strength, whereas samples (B) and (C) were found to be deformed to large deformation strains. High strength of samples A may be attributed to their thick cell walls resulting from the large- in number- small in size existing pores that inhibit the dislocation glide [4] and the high volume fraction of the

solid material making the foam [5]. Some pores of low density samples that contain large pore sizes fail during tension resulting in a localized damage. As the pores elongate in the loading direction, many cracks initiate and continue from one cell to another leading to the entire fracture.

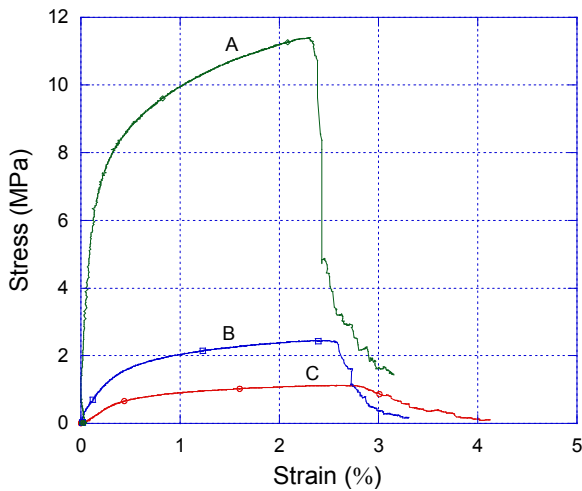


Fig. 4. Tensile stress-strain curves of samples A, B and C having pore sizes of 150, 300 and 600 μm , respectively.

Effect of Porosity

Balshin et al. [6] put an empirical relationship correlating the stress with the porosity has the form of eq.1

$$\sigma = \sigma_0(1-p)^K \quad (1)$$

where K is an empirical constant, depends on the material and fabrication method. Boccaccini et al. [7] correlated the empirical constant K with the stress concentration around the pores. The stress concentration factor depends on the pore geometry and orientation about the direction of the applied stress.

Dehoff et al. [8, 9] found out a correlation between the yield strength and the porosity as well. Two types of yielding occur. At low porosity level, the yield strength decreases linearly with increasing porosity, and the yield strength over the critical porosity level drastically decreases with increasing the porosity. In the same way, Young's modulus was found to be influenced by the porosity. The Young's modulus decreases exponentially as the hollow microspheres increase [10, 11, 12].

In the model of Gibson and Ashby [13], the foam's modulus of elasticity is given by eq. 2

$$\frac{E}{E_0} = C\left(\frac{\rho}{\rho_0}\right)^n = C(1-p)^n \quad (2)$$

where E is the modulus of the foam, p is the porosity, E_0 and ρ_0 are the modulus and density of the dense material, respectively. The constants C and n depend on the foam's

microstructure. n takes values between 1 and 4 giving a wide range for $\frac{E}{E_0}$ at a given density [14].

Determination of mean fracture stress

We measured statistically the mean fracture stress of the individual cells by using a Weibull distribution Analysis. Recall the tensile stress-strain curve, we find the foams fail in a successive way as soon as the applied load exceeds the maximum strength of the foam struts. The zigzag line, shown in Fig. 5, represents the fracture of foam's cell walls taking place randomly from one cell to its neighbouring starting from the weakest one. Each knick represents the fracture of one cell wall or strut. For example σ_1 is considered as the fracture stress of the first wall of the weakest cell in the structure, σ_2 is the fracture stress of the second cell and so on, as shown in Fig. 5.

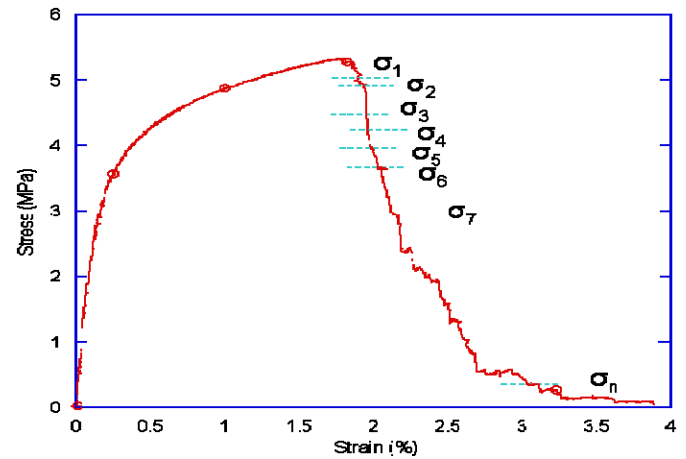


Fig. 5. Fracture stress determination from a tensile stress-strain curve of a foam sample.

Applying the Weibull distribution described by eq. 3, 4

$$F = 1 - \exp\left\{-\left(\frac{\sigma}{\sigma_0}\right)^m\right\} \quad (3)$$

$$\ln \ln(1-F)^{-1} = m \ln \sigma - m \ln \sigma_0 \quad (4)$$

where F is the probability of survival, σ is the stress, σ_0 is the characteristic stress or the scale parameter and m is the shape parameter. By plotting $\ln \ln(1-F)^{-1}$ vs $\ln \sigma$, as shown in Fig. 8, m and σ_0 can be determined. It can be seen that samples of small cell wall thickness fail at lower stresses than those of thicker ones.

In Fig. 7 the dependence of the ultimate tensile strength (σ_{UTS}) and yield stress (σ_y) on the porosity and cell wall thickness is elucidated. Improved mechanical properties can be achieved by increasing the thickness of foam's cell wall.

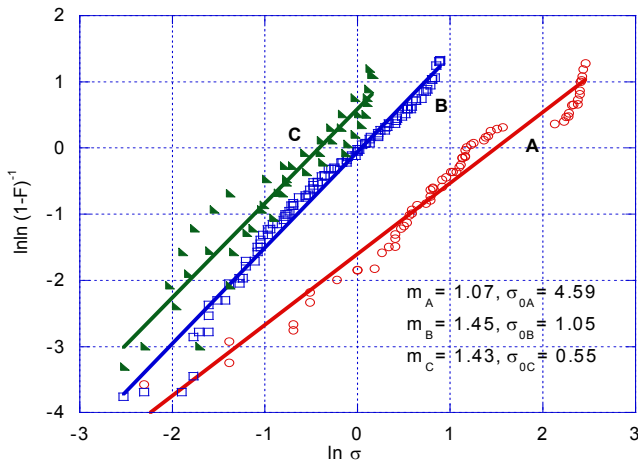


Fig. 6. Determination of shape (m) and scale parameters (σ_0) by using the Weibull distribution.

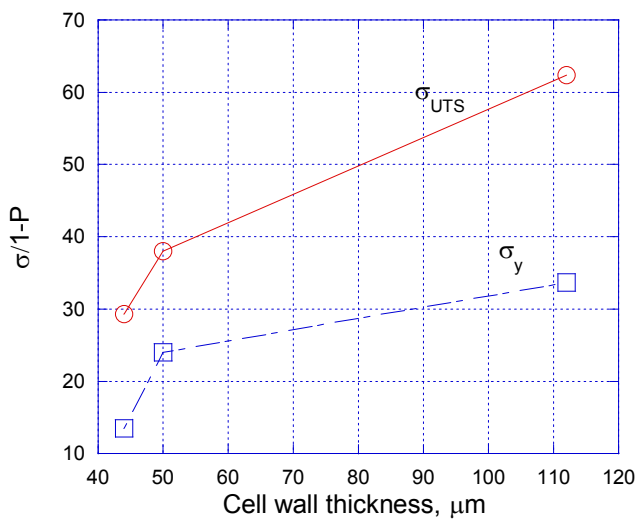


Fig. 7. Ultimate tensile strength (σ_{UTS}) and yield stress (σ_y) as a function of foam's cell wall thickness.

Electrical Resistivity

Electrical resistivity is an intrinsic property of a resistor material that allows for the calculation of the electrical resistance, R , expressed in ρ , of a homogeneous conductor with a regular cross-sectional area, A , expressed in square cm, and a length, L in cm. R is given by the following equation, where the proportional quantity, ρ , is the electrical resistivity of the material, expressed in ohm .cm:

$$R = \rho \frac{l}{A} \tag{5}$$

Electrical resistivity ρ (Greek: rho) is defined by,

$$\rho = \frac{E}{J} \tag{6}$$

Where ρ is the static resistivity (measured in ohm-meters, Ω -m), E is the magnitude of the electric field (measured in volts per meter, V/m), J is the magnitude of the current

density (measured in amperes per square meter, A/m^2), and E and J are both inside the conductor. Many resistors and conductors have a uniform cross section with a uniform flow of electric current and are made of one material. In this case, the above definition of ρ leads to:

$$R = \rho \frac{l}{A} \tag{7}$$

Where (R) is the electrical resistance of a uniform specimen of the material (measured in ohms, Ω)

In this work using electrical resistivity of each steel foams with different densities and average pore sizes, namely 150, 300 and 600 μ m respectively, foam was determined using a foam cut from the same sample as the corresponding heating element. Direct electric current was passed through a rectangular length of foam. The voltage and current were recorded, and the resistance calculated using Ohm's law. The physical dimensions of the test specimen, length, width, and thickness, were measured. From these parameters, the resistivity was determined using Equation (5).

A is the cross sectional area of the sample
 L is the distance between the voltage probes, equivalent to the length.

R is the electric resistance of sample between voltage probes. The figure .8 shows the Electrical resistivity measurement setup using four point Probe, while figure .8 shows the Electrical resistivity measured for three samples with different skins.

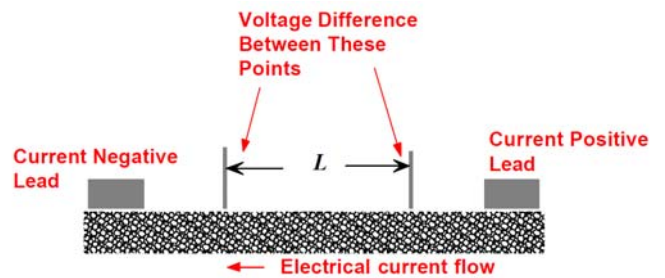


Fig 8. Electrical resistivity measurement setup using four point Probe.

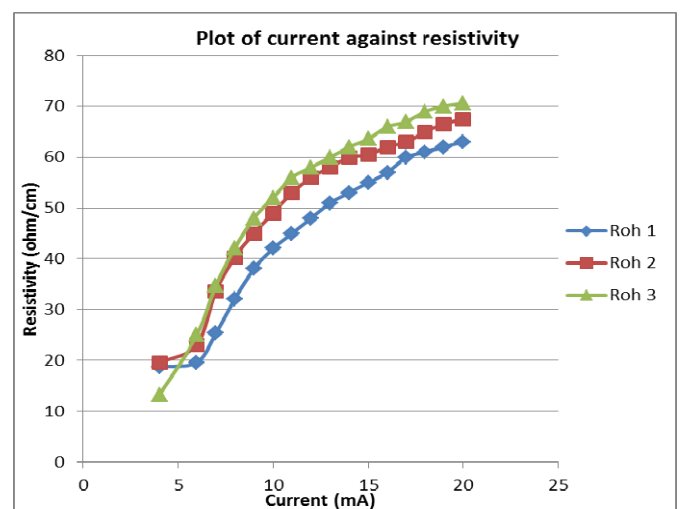


Fig 9. Electrical resistivity measurement setup using four point Probe.

III. CONCLUSION

The main aim is to develop lightweight structures which are stiff, strong, able to absorb Large amount of energy and cheap for application in the transport and construction industries. For example, the firewall between the engine and passenger compartment of an automobile must have adequate mechanical strength, good energy and sound absorbing properties, and adequate fire redardance. Metal foams provide all of these features, and axe under serious consideration for this applications by a number of automobile manufacturers in this paper lightweight structures had been done and tensile strength had been tested for all samples the strain Despite foams increasingly importance, studies correlating their mechanical properties with the microstructure are still limited. Then tested the electrical properties using four point probe and the result are shown in fingers for different samples.

REFERENCES

- [1] J. Banhart, *Progress in Materials Science*, vol.46, 2001, pp.559-632.
- [2] K., Lee, K., Lewandowski. "Effects of Microstructural characteristics on mechanical properties of open-cell nickel foams," *Journal of Materials Science and Technology*, vol. 21, 2005, pp.1355-1358.
- [3] W., Masahiro, "Processing of Metal Foams using Slurry Technique," *Chemical Society Japan*, 54 (7).
- [4] G. J. C. Carpenter, Z.S., Wronski, M.W. Phaneuf, "TEM study of nanopores and the embrittlement of CVD nickel foam," *Journal of Materials Science and Technology*, vol. 20, 2004, pp. 1421-1426.
- [5] G. Subhash, Q. Liu, X. Lin, "Quasistatic and high strain rate uniaxial compressive response of polymeric structural foams", *International Journal of Impact Engineering*, vol. 32,2006, pp 1113–1126.
- [6] M. Balshin, Y. Doklady, *Akademic Science USSR*, vol. 67, 1949,pp 831.
- [7] A.R. Boccaccini, G. Ondracek, E. Mombello, *Journal of Materials Science Letters*, vol. 14, 1995, pp 534.
- [8] R.T. Dehoff, J.P. Gillard, *Powder Metall.*, vol. 5, eds. H.H. Hausner: Plenum Press, NY, 1971, pp. 281.
- [9] J.A. Lund,1984. *Int. J. Powder Metall., Powder Tech.* vol. 20, 1984, pp.141.
- [10] V.D. Krstic, W.H. Erickson "A model for the porosity dependence of Young's modulus in brittle solids based on crack opening displacement," *Journal of Materials Science*, vol. 22, 1987, pp 2881-2886.
- [11] M.A. El- Hadek, H.V Tippur2002. "Simulation of porosity by microballoon dispersion in epoxy and urethane: mechanical measurements and models," *Journal of Materials Science*, vol. 37, 2002, pp 1649-1660.
- [12] E.M. Wouterson, Y.C. Freddy, X.H. Boey, S.C. Wong, "Specific properties and fracture toughness of syntactic foam: Effect of foam structures," *Composites Sci. Technol.* Vol. 65, 2005, pp 1840- 1850.
- [13] L.J. Gibson, M.F. Ashby, *Cellular Solids: Structure and Properties*. Oxford: Pergamon Press, 1988.
- [14] F.G. Torres, S.N. Nazhat, S.H. Fadzullah,, V. Maquet, A.R. Boccaccini,"Mechanical Properties and Bioactivity of Porous PLGA/TiO2 Nanoparticl-filled Composites for Tissue Engineering Scaffolds," *Composites Sci. Technol..and Computer Science: World Congress on Engineering and Computer Science 2009*, pp. 1–7